TRANSACTIONS ON ELECTRICAL AND ELECTRONIC MATERIALS
Vol. 18, No. 2, pp. 74-77, April 25, 2017

Regular Paper

pISSN: 1229-7607 eISSN: 2092-7592
DOI: https://doi.org/10.4313/TEEM.2017.18.2.74
OAK Central: http://central.oak.go.kr

Chemical Reaction on Etched TaNO Thin Film as O_2 Content Varies in CF_4/Ar Gas Mixing Plasma

Jong Chang Woo
Department of Electronic Automation Engineering, Daeduk University, Daejeon 34111, Korea

Chang-Il Kim†
School of Electrical and Electronics Engineering, Chung-Ang University, Seoul 06974, Korea

Received September 20, 2016; Accepted November 22, 2016

In this work, we investigated the etching characteristics of TaNO thin films and the selectivity of TaNO to SiO_2 in an O_2/CF4/Ar inductively coupled plasma (ICP) system. The maximum etch rate of TaNO thin film was 297.1 nm/min at a gas mixing ratio of O_2/CF_4/Ar (6:16:4 sccm). At the same time, the etch rate was measured as a function of the etching parameters, such as the RF power, DC-bias voltage, and process pressure. X-ray photoelectron spectroscopy analysis showed the efficient destruction of the oxide bonds by the ion bombardment, as well as the accumulation of low volatile reaction products on the etched surface. Based on these data, the ion-assisted chemical reaction was proposed as the main etch mechanism for the CF_4-containing plasmas.

Keywords: TaNO, ICP, XPS

1. INTRODUCTION

Until now, many researchers have studied the properties of TaNO thin films [1-5]. Their application for thin film resistors is restricted because their resistivity changes suddenly when the nitrogen partial pressure is increased, and because TaNO thin films have a variety of crystal structures. The range of resistivity, that can be obtained by changing the partial pressure, is not sufficient for all types of embedded passive resistors. Therefore, different methods are needed to allow stable resistivity control. In addition, a fine process with a relatively high etch rate, high selectivity, strict control of CD (critical dimension) variation, a steep profile, and no recessed under layer is needed when the feature size of the gate is below several nanometers.

To date, the etch characterization of TaNO thin film hasn't been studied using a high density plasma. S. Beck obtained a steep profile of the TiN/TaN stack using oxide mask and BCl_3 and/or Cl_2/HBr. However, during the high-*k* etch process with BCl_3 chemistry, TaN thin film was removed laterally and formed a undercut profile [6-8]. In our experiment, O_2/CF_4/Ar plasma was selected as the etching gas chemistry because O_2/CF_4/Ar plasma was widely used due to its high selectivity and possible formation of a passivation layer. However, the etch mechanism of TaNO thin film in O_2/CF_4/Ar has not been studied.

In this research, the etch properties of TaNO thin films and the surface reaction between TaNO thin film and O_2/CF_4/Ar plasma were investigated with an inductively coupled plasma (ICP) etch system. In order to understand the effects of input parameters on the etch rates of TaNO thin film and selectivity respect to SiO_2, we investigated the variation of input parameters such as O_2/CF_4/Ar gas mixing ratio, RF power, DC-bias voltage, and process pressure. X-ray photoelectron spectroscopy (XPS) was performed to understand the variations in the chemical states of TaNO thin film when the TaNO thin film surface was exposed in O_2/CF_4/Ar plasma.

† Author to whom all correspondence should be addressed:
E-mail: cikim@cau.ac.kr

2. EXPERIMENTS

The TaNO thin films were fabricated on standard 8 inch silicon wafers with a resistivity of 15 ~ 25 Ohm · cm. The TaNO thin film produced by the oxidation of deposited TaN films at 400℃ had a

Table 1. Process conditions.

Gas mixture (sccm)	$O_2/CF_4/Ar(0\sim9:16:4)$
RF power (W)	500 ~ 800
DC-bias voltage (V)	-150 ~ -300
Process pressure (Pa)	1 ~ 3

final thickness of about 160 nm. The etching experiments were performed in a ICP system [9]. The reactor consisted of a cylindrical chamber with a 26 cm diameter and two power generators. A 13.56 MHz power generator was connected to a 3.5 turn copper coil to generate the ICP. Another 13.56 MHz power generator was attached to the substrate electrode to control the DC-bias voltage. The etching characteristics of the TaNO thin films were investigated as a function of the $O_2/CF_4/Ar$ gas mixing ratio. In addition, the plasma etching of the TaNO thin films was investigated by changing the etching parameters listed in Table 1. The etch rate was measured by a surface profiler (α-step 500 KLA Tencor). The compositional changes on the etched TaNO surface were investigated using XPS (Thermo VG Scientific SIGMA PROBE). The spectra were plotted by counting the photo electrons at kinetic energy intervals of 0.1 eV. The detailed information of the inner region of the film was provided by the spectra recorded at 90°. All of the samples for the XPS analysis were bare TaNO thin films without any photo-resist patterns and the size of the samples and etching time were 1×1 cm^2 and 10 sec, respectively.

3. RESULTS AND DISCUSSION

3.1 Effect of O_2 content in CF_4/Ar gas mixing and RF power

For the characterization of the TaNO thin film was systematically investigated as functions of the $O_2/CF_4/Ar$ gas mixing ratio, RF power, DC-bias voltage, and process pressure. Figure 1(a) shows the etch rate of the TaNO thin film as a function of the $O_2/CF_4/Ar$ plasma gas mixing ratio. The other process conditions, viz. the RF power, DC-bias voltage, process pressure, and substrate temperature, were maintained at 700 W, - 250 V, 2 Pa, and 40℃, respectively. As the O_2 content in the CF_4/Ar gas plasma increased, the etch rates and selectivity of the TaNO thin films increasesd The maximum etch rate of TaNO thin film was 297.1 nm/min at $O_2/CF_4/Ar$ (=6:16:4 sccm) [10,11]. This implies that, for a given range of experimental conditions, the chemical reactions were more effective than the physical etch pathway. Figure 1(b) shows the effect of the RF power on the etch rates of TaNO thin film in the $O_2/CF_4/Ar$ plasma. As the RF power applied to the ICP coil was raised from 500 to 800 W, the other process conditions, viz. DC-bias voltage, process pressure, and substrate temperature, were maintained at - 250 V, 2 Pa, and 40℃, respectively. The etch rate of the TaNO thin film increased from 184.8 to 333 nm/min. This etch rate behavior with increasing RF power may be explained by the acceleration of both the physical and chemical etching pathways as the volume densities and fluxes of ions and fluorine atoms increased.

3.2 Effect of process pressure and DC-bias voltage

Figure 2(a) shows the etch rate of TaNO thin film as a function of the process pressure in the $O_2/CF_4/Ar$(=6:16:4 sccm) plasma. As the process pressures increased from 1 to 3 Pa, the other process conditions, viz. the RF power, DC-bias voltage, and substrate temperature, were maintained at 700 W, - 250 V, and 40℃, respectively. The TaNO thin film etch rate decreased from 371.4 to 244.4 nm/min. This decrease in process pressure reduces the density of the chemically active species, which reduces the chemical reaction. However, since the mean free path and ion energy increases with decreasing process pressure, the ion stimulated

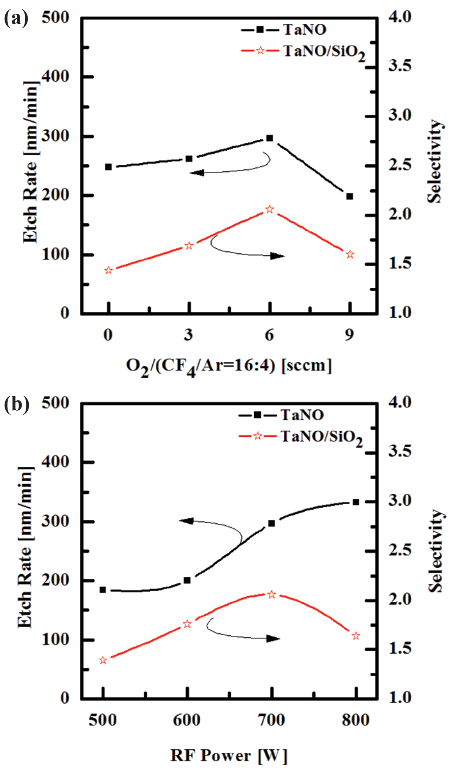

Fig. 1. Etch rates of TaNO and the selectivity of TaNO to SiO_2 as a function of the $O_2/CF_4/Ar$ gas mixing ratio and RF power.

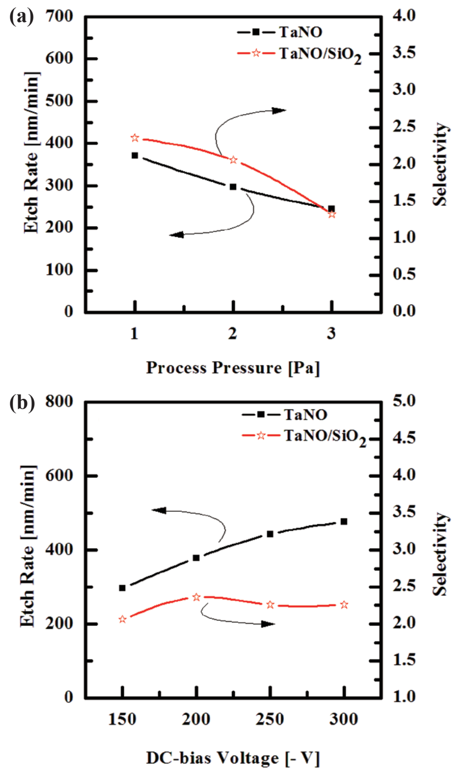

Fig. 2. Etch rates of TaNO and the selectivity of TaNO to SiO_2 as a function of the process pressure and DC-bias voltage.

desorption of the reaction products increased and the fraction of free surface available for the chemical reaction decreased. As a result of the effect of the pressure on the etch rate of the TaNO thin film, the etch process is limited by the supply of the chemical source, and therefore, the etch rate of the TaNO thin film decreases with increasing process pressure [16,17]. The TaNO thin film etch rates are shown in Fig. 2(b) as a function of the DC-bias voltage. As the DC-bias voltage increases from - 150 to - 300 V, the other process conditions, viz. the RF power, process pressure, and substrate temperature, were maintained at 700 W, 2 Pa, and 40℃, respectively. The TaNO thin films etch rate increased from 297.1 to 476.7 nm/min. This etch rate increase is attributed to the increase of the mean ion energy. This results in a sputtering yield increase for both TaNO thin film and the reaction products [12-15].

In our opinion, the domination of the chemical reactions may be explained by the following factors. Since the melting point of TaF_5 is about 229℃, the chemical pathway domination may be related to its lack of volatility. As a result, radical and ion densities increased with increasing RF power. The molecular bonds were broken by the ions bombarding the TaNO thin film surface. Therefore, chemical reactions were frequently generated in the plasma due to the higher ion density and increased number of broken molecular bonds. The etched byproducts were easily evaporated by these physical and chemical phenomena. This conclusion is supported by the data shown in Figs. 1 and 2.

3.3 XPS analysis

In order to analyze the surface chemical state in detail, XPS narrow scan analysis was performed as a function of O_2 content in CF_4/Ar(=16:4 sccm) plasma. The Ta 4f narrow scan spectra taken at a 90° angle were obtained from the TaNO surfaces. As shown in Fig. 3, mono peaks at the binding energy (B. E.) of 26.1 eV and 27.6 eV corresponded to Ta $4f_{5/2}$ and Ta $4f_{7/2}$ as reported by C. Atanassova et. al [18-20]. As shown in Fig. 3(a), the narrow scan spectra appeared in the peaks obtained from the TaNO film as deposited, and after etching. When the TaNO thin films were exposed to the O_2/CF_4/Ar(=0~9:16:4 sccm) plasma, the Ta 4f core peak decreased in intensity. For the O_2/CF_4/Ar(=0:16:4 sccm) plasma as shown in Fig. 3(b), the Ta 4f peak can be decomposed into two peaks corresponding to the Ta-N or Metal bond (25.85 eV) and the Ta-O_x bond (27.6 eV). These binding energies are in agreement with the reported values [19]. The intensity of these peaks decreased when increasing the O_2/CF_4/Ar(=6:16:4 sccm) mixing ratio, as shown in Figs. 3(c)~(d). The Ta 4f peak can also be decomposed into three peaks corresponding to the Ta-N or Metal bond (25.85 eV), the Ta-O_x bond (27.6 eV), and the Ta_2-O_5 bond (28.2 eV, 28.3 eV). Also, a new peak appeared at the Ta_2-O_5 peak. The etching processes in the CF_4/Ar(=16:4 sccm) plasma and O_2/CF_4/Ar(=6:16:4 sccm) caused a noticeable decrease in the Ta 4f peak. This can be attributed to the destruction of the oxide bonds by ion bombardment. This chemical shift indicated that a chemical reaction occurred between Ta, O and F, resulting in the formation of Ta-F bonds on the surface [19-21].

Figure 4 shows the XPS narrow scan spectra for O 1s taken at a 90° angle. These TaNO surface spectra were taken after etching in the O_2/CF_4/Ar(=0~9:16:4 sccm) gas mixture. As shown in Fig. 4(a), the narrow scan spectra appeared at the peaks obtained from the TaNO film as deposited and after etching. The peak at 530.6 eV corresponds to the O 1s bond. When the TaNO thin film was exposed to the O_2/CF_4/Ar (=0:16:4 sccm) plasma and the O_2/CF_4/Ar (=6:16:4 sccm) plasma, the O 1s core peak decreased in intensity. For the O_2/CF_4/Ar (=0:16:4 sccm) plasma TaNO thin film (as shown in Fig. 4(b)), the O 1s peak can be decomposed into three peaks corresponding to the O-Ta (530.6 eV), O-O (531.75 eV), and O-F (533.1 eV) bonds. As shown in Figs. 4(c)~(d) for O 1s, the O 1s peak can be decomposed into three peaks corresponding to the O-Ta

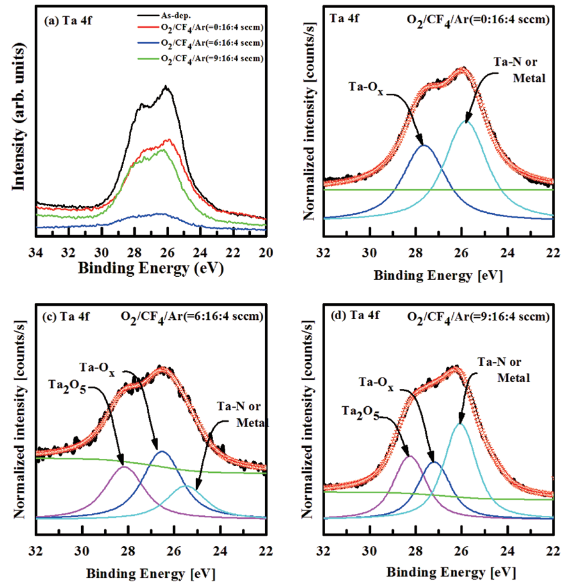

Fig. 3. Ta 4f XPS spectra of TaNO surface etched with O_2/CF_4/Ar gas mixing ratio at take off angle of 90°. (a) Narrow scan, (b) O_2/CF_4/Ar=0:16:4 sccm, (c) O_2/CF_4/Ar=6:16:4 sccm, and (d) O_2/CF_4/Ar=9:16:4 sccm.

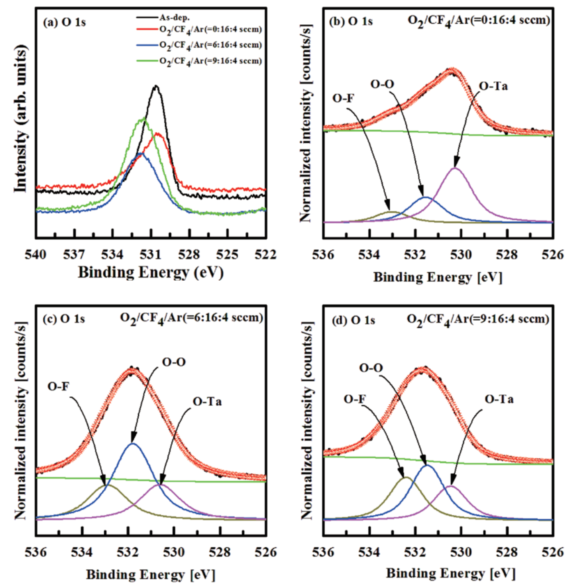

Fig. 4. O 1s XPS spectra of TaNO surface etched with O_2/CF_4/Ar gas mixing ratio at take off angle of 90°. (a) Narrow scan, (b) O_2/CF_4/Ar=0:16:4 sccm, (c) O_2/CF_4/Ar=6:16:4 sccm, and (d) O_2/CF_4/Ar=9:16:4 sccm.

(530.6 eV, 530.45eV), O-O (531.75 eV, 531.5 eV), and O-F (532.9 eV, 532.4 eV) bonds. After etching the TaNO thin film in the plasmas, the shoulder peak of O-F (532.9 eV, 532.4 eV) decreased significantly. However, in the TaNO thin film spectra that were etched in the O_2/CF_4/Ar (=0:16:4 sccm) and O_2/CF_4/Ar(=6:16:4 sccm) plasmas, the O 1s peak intensities corresponding to the O-Ta and O-O bonds decreased owing to the formation of O-F bonds [18]. The dramatic increase in the number of O-F bonds was due to the effective dissociation of the Ta-O bonds by the ion bombardment. Based on the XPS results, it was revealed that Ta and O were removed by the chemical reactions with the F radicals and by the physical bombardment of the Ar ions [18,19].

Figure 5 shows the XPS narrow scan spectra for N 1s taken at a 90° angle. These TaNO surface spectra were taken before and after

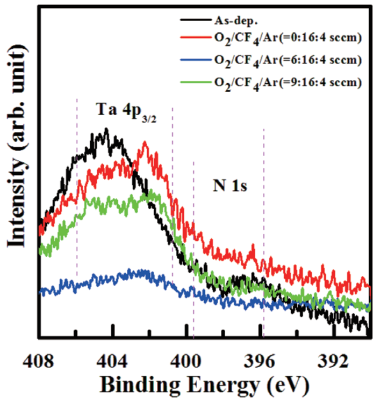

Fig. 5. N 1s XPS narrow scan spectra of TaNO surface etched with O_2/CF_4/Ar gas mixing ratio at a take off angle of 90°.

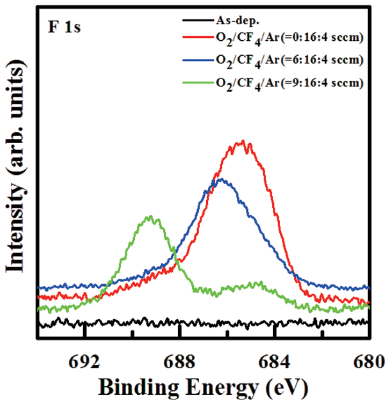

Fig. 6. F 1s XPS narrow scan spectra of TaNO surface etched with O_2/CF_4/Ar gas mixing ratio at a take off angle of 90°.

etching in the O_2/CF_4/Ar gas mixture at a fixed RF power of 700 W, a DC-bias voltage of - 250 V, a process pressure of 2 Pa, and a substrate temperature of 30℃. We could not identify the N 1s peaks from 396 eV to 400 eV. Because the O-F bond is removed during the etching process, the intensity of the N 1s peak did not appear to be nearly that of the Ta $4p_{3/2}$ peak [18-20]. The F 1s photoelectron peaks obtained from the etched sample are shown in Fig. 6. The XPS binding energy of 685.6 eV was assigned to F 1s as a result of the less volatile Ta-F_x. This lead to an etch rate increase with increasing amounts of O_2 content in the CF_4/Ar plasma. This shift to higher energy was due to the chemical reaction [20,21].

4. CONCLUSIONS

We investigated the etching characteristics of TaNO thin films using an ICP system. The etching characteristics (including the etch rates) and selectivity of TaNO thin films were investigated as functions of the etching parameters. The maximum etch rate of the TaNO thin film was 297.1 nm/min in O_2/CF_4/Ar(=6:16:4 sccm) plasma. As the O_2 fraction in the O_2/CF_4/Ar plasma increased from 0 to 9 sccm, the TaNO etch rate increased from 0 to 6 sccm. However, the TaNO etch rate decreased with the further addition of O_2 gas. The etch rates of the TaNO thin films increased with increasing RF power, and DC-bias voltage, but decreased with increasing process pressure. Ion bombardment was required to enhance the etching characteristics due to the relatively low volatility of the by products formed during etching by the O_2/CF_4/Ar plasma. The chemical states of the etched TaNO films were investigated using XPS. The etching mechanism of the TaNO thin film can be explained as follows: Ta interacted with the F radicals in the O_2 containing plasmas, but remained at the surface due to the low volatility of TaF_x. This can be effectively removed with the help of ion bombardment. These results agree with the general energy dependency of ion enhanced chemical etching yields.

REFERENCES

[1] R. J. Gaboriaud, F. Paumier, F. Pailloux, and P. Guerin, *Mater. Sci. Eng. B*, **109**, 34 (2004). [DOI: http://org/10.1016/j.mseb.2003.10.023]

[2] L. Kang, B. H. Lee, W. Qi, Y. Jem, R. Nich, S. Gopalan, K. Onishi, and J. C. Leen, *IEEE Electron. Dev. Lett.*, **21**, 181 (2000).

[3] K. Pelhos, V. M. Donnelly, A. Kornblit, M. L. Green, R. B. Van Dover, L. Manchanda, Y. Hu, M. Morris, and E. Bower, *J. Vac. Sci. Technol. A*, **19**, 1361 (2001). [DOI: http://org/10.1116/1.1349721]

[4] E. S. Lee, *Trans. Electr. Electron. Mater.*, **12**, 68 (2011). [DOI: https://doi.org/10.4313/TEEM.2011.12.2.68]

[5] H. Chakraborty, A. Sinha, S. Chabri, and N. Bhowmik, *Trans. Electr. Electron. Mater.*, **14**, 121 (2013). [DOI: http://org/10.4313/TEEM.2013.14.3.121]

[6] M. Stavrev, D. Fischer, A. Preu, B. C. Wenzel, and N. Mattern, *Microelectro. Eng.*, **33**, 269 (1997). [DOI: http://org/10.1016/S0167-9317(96)00054-8]

[7] J. Zhang, F.H.B. Lima, M. H. Shao, K. Sasaki, J. X. Wang, J. Hanson, and R. R. Adzic, *J. Phys. Chem B*, **109**, 22701 (2005). [DOI: http://org/10.1021/jp055634c]

[8] C. Q. Jiao, R. Nagpal, and P. Haaland, *Chem. Phys. Lett.*, **265**, 242 (1997). [DOI: http://org/10.1016/S0009-2614(96)01419-4]

[9] G. H. Kim, C. I. Kim, and A. M. Efremov, *Vacuum*, **79**, 231 (2005). [DOI: http://org/10.1016/j.vacuum.2005.03.012]

[10] W. S. Hwang, J. Chen, W. J. Yoo, and V. Bliznetsov, *J. Vac. Sci. Technol. A*, **23**, 964 (2005). [DOI: http://org/10.1116/1.1927536]

[11] J. Tonotani, T. Iwamoto, F. Sato, K. Hattori, S. Ohmi, and H. Iwai, *J. Vac. Sci. Technol. B*, **21**, 2163 (2003). [DOI: http://org/10.1116/1.1612517]

[12] K. J. Park, K. H. Kim, W. M. Lee, H. Chae, I. S. Han, and H. D. Lee, *Trans. Electr. Electron. Mater.*, **10**, 35 (2009). [DOI: http://org/10.4313/TEEM.2009.10.2.035]

[13] H. J. Lee, B. S. Kwon, H. W. Kim, S. I. Kim, D. G. Yoo, J. H. Boo, and N. E. Lee, *Jpn. J. Appl. Phys.*, **47**, 6960 (2008). [DOI: http://org/10.1143/JJAP.47.6960]

[14] M. H. Shin, S. W. Na, N. E. Lee, T. K. Oh, J. Kim, and T. Lee, J. Ahn, *Jpn. J. Appl. Phys.*, **44**, 5811 (2005). [DOI: http://org/10.1143/JJAP.44.5811]

[15] H. K. Chiu, T. L. Lin, Y. Hu, K. C. Leou, H. C. Lin, M. S. Tsai, and T. Y. Huang, *J. Vac. Sci. Technol. A*, **19**, 455 (2001). [DOI: http://org/10.1116/1.1342866]

[16] M. Efremov, D. P. Kim, and C. I. Kim, *J. Vac. Sci. Technol. B*, **75**, 133 (2004).

[17] E. Jud, M. Tang, and Y. M. Chiang, *J. Appl. Phys.*, **103**, 114108 (2008). [DOI: http://org/10.1063/1.2937900]

[18] E. Atanassova, G. Tyuliev, A. Paskaleva, D. Spassov, and K. Kostov, *Appl. Surf. Sci.*, **225**, 86 (2004). [DOI: http://org/10.1016/j.apsusc.2003.09.040

[19] X. Zhao, N. P. Magtoto, and J. A. Kelber, *Thin Solid Films*, **478**, 188 (2005). [DOI: http://org/10.1016/j.tsf.2004.10.042]

[20] N. Kirchner, K. H. Hallmeier, R. Szargan, T. Raschke, C. Radehaus, and G. Wittstock, *Electroanalysis*, **19**, 1023 (2007). [DOI: http://org/10.1002/elan.200703832]

[21] S.H.N. Lim, D. G. McCulloch, M.M.M. Bilek, D. R. McKenzie, J. Plessis, M. V. Swain, and R. Wuhrer, *Surf. Coat. Technol.*, **201**, 396 (2006). [DOI: http://org/10.1016/j.surfcoat.2005.11.141]